

Arylpalladium Complexes with a Silsesquioxane Ligand. Preparation and Structures in the Solid State and in Solution

Neli Mintcheva, Makoto Tanabe, and Kohtaro Osakada*

Chemical Resources Laboratory (R1-3), Tokyo Institute of Technology, 4259 Nagatsuta, Midori-ku, Yokohama 226-8503, Japan

Received November 15, 2006

The reaction of the incompletely condensed silsesquioxane (c-C₅H₉)₇Si₇O₉(OH)₃ with [Pd(C₆H₃Me₂-2,4)(I)(bpy)] produced a complex with a Pd–O bond, [Pd(C₆H₃Me₂-2,4){(c-C₅H₉)₇Si₇O₁₀(OH)₂}(bpy)]. Palladium complexes having a silsesquioxane ligand, [Pd(Ar){R₇Si₇O₁₀(OH)₂}(tmeda)] (Ar = C₆H₅, C₆F₅, C₆H₃F₂-2,4; R = c-C₅H₉, i-C₄H₉), were prepared by the reaction of the silsesquioxane R₇Si₇O₉(OH)₃ with arylpalladium iodo complexes, [Pd(Ar)(I)(tmeda)] (tmeda = *N,N,N',N'*-tetramethylethylenediamine), in the presence of Ag₂O. These complexes were characterized by multinuclear (¹H, ¹³C{¹H}, ¹⁹F{¹H}, and ²⁹Si{¹H}) NMR spectroscopy, and the structure of [Pd(C₆F₅){(c-C₅H₉)₇Si₇O₁₀(OH)₂}(tmeda)] was determined by X-ray crystallography. Temperature-dependent ¹H and ¹⁹F{¹H} NMR spectra revealed the dynamic behavior of the complexes on the NMR time scale.

Introduction

Transition-metal complexes having an incompletely condensed silsesquioxane as a ligand are considered as suitable soluble model compounds for silica-supported catalysts in organic synthesis.¹ Such metallasilsesquioxanes that contain early transition metals may act as molecular catalysts in polymerization epoxidation and the metathesis reactions of alkenes.² Metal clusters protected by silsesquioxanes and metallasilsesquioxanes immobilized on polysiloxanes catalyze olefin epoxidation and CH₄ and NH₃ oxidation reactions.³ Palladium complexes with silsesquioxane–amine ligands and cubic silsesquioxanes have

been employed as the precursors of silica-based catalysts with encapsulating Pd oxide nanoparticles.⁴ Vogt and co-workers reported palladium complexes having mono- and bidentate phosphite ligands functionalized with silsesquioxanes.⁵ There have been no reports on palladium complexes with O-bonded silsesquioxane ligands derived from incompletely condensed silsesquioxanes. Recently, several research groups, including ours, identified Pt complexes with mono- and bidentate silsesquioxane ligands.⁶ Although Pt and Pd complexes with O-bonded alkoxo^{7,8} and aryloxo⁹ ligands have been widely investigated during the last few decades, the corresponding silanolate complexes having a M–O–Si bond (M = Pd, Pt) are much rarer.^{10–12} These silsesquioxane or silanolate complexes of Pd and Pt mostly contain phosphines as auxiliary ligands. In this paper, we present our results for the preparation,

* To whom correspondence should be addressed. E-mail: kosakada@res.titech.ac.jp.

(1) (a) Feher, F. J.; Newman, D. A.; Walzer, J. F. *J. Am. Chem. Soc.* **1989**, *111*, 1741–1748. (b) Feher, F. J.; Newman, D. A. *J. Am. Chem. Soc.* **1990**, *112*, 1931–1936. (c) Feher, F. J.; Budzichowski, T. A.; Blanski, R. L.; Weller, K. L.; Ziller, J. W. *Organometallics* **1991**, *10*, 2526–2528. (d) Duchateau, R.; Dijkstra, T. W.; van Santen, R. A.; Yap, G. P. A. *Chem. Eur. J.* **2004**, *10*, 3979–3990.

(2) (a) Feher, F. J.; Budzichowski, T. A. *Polyhedron* **1995**, *14*, 3239–3253. (b) Duchateau, R.; Abbenhuis, H. C. L.; van Santen, R. A.; Meetsma, A.; Thiele, S. K.-H.; van Tol, M. F. H. *Organometallics* **1998**, *17*, 5663–5673. (c) Abbenhuis, H. C. L. *Chem. Eur. J.* **2000**, *6*, 25–32. (d) Wada, K.; Itayama, N.; Watanabe, N.; Bundo, M.; Kondo, T.; Mitsudo, T. *Organometallics* **2004**, *23*, 5824–5832.

(3) (a) Wada, K.; Nakashita, M.; Yamamoto, A.; Mitsudo, T. *Chem. Commun.* **1998**, 133–134. (b) Krijnen, S.; Abbenhuis, H. C. L.; Hanssen, R. W. J. M.; van Hooff, J. H. C.; van Santen, R. A. *Angew. Chem., Int. Ed.* **1998**, *37*, 356–358. (c) Maxim, N.; Magusin, P. C. M. M.; Kooyman, P. J.; van Wolput, J. H. M. C.; van Santen, R. A.; Abbenhuis, H. C. L. *Chem. Mater.* **2001**, *13*, 2958–2964. (d) Wada, K.; Yamada, K.; Kondo, T.; Mitsudo, T. *Chem. Lett.* **2001**, 12–13. (e) Maxim, N.; Overweg, A.; Kooyman, P. J.; van Wolput, J. H. M. C.; Hanssen, R. W. J. M.; van Santen, R. A.; Abbenhuis, H. C. L. *J. Phys. Chem. B* **2002**, *106*, 2203–2209. (f) Murugavel, R.; Davis, P.; Shete, V. S. *Inorg. Chem.* **2003**, *42*, 4696–4706. (g) Skowronska-Ptasinska, M. D.; Vorstenbosch, M. L. W.; van Santen, R. A.; Abbenhuis, H. C. L. *Angew. Chem., Int. Ed.* **2002**, *41*, 637–639.

(4) (a) Naka, K.; Itoh, H.; Chujo, Y. *Nano Lett.* **2002**, *2*, 1183–1186. (b) Wada, K.; Yano, K.; Kondo, T.; Mitsudo, T. *Catal. Today* **2006**, *117*, 242–247.

(5) (a) van der Vlugt, J. I.; Fioroni, M.; Ackerstaff, J.; Hanssen, R. W. J. M.; Mills, A. M.; Spek, A. L.; Meetsma, A.; Abbenhuis, H. C. L.; Vogt, D. *Organometallics* **2003**, *22*, 5297–5306. (b) van der Vlugt, J. I.; Ackerstaff, J.; Dijkstra, T. W.; Mills, A. M.; Kooijman, H.; Spek, A. L.; Meetsma, A.; Abbenhuis, H. C. L.; Vogt, D. *Adv. Synth. Catal.* **2004**, *346*, 399–412.

(6) (a) Abbenhuis, H. C. L.; Burrows, A. D.; Kooijman, H.; Lutz, M.; Palmer, M. T.; van Santen, R. A.; Spek, A. L. *Chem. Commun.* **1998**, 2627–2628. (b) Quadrelli, E. A.; Davies, J. E.; Johnson, B. F. G.; Feeder, N. *Chem. Commun.* **2000**, 1031–1032. (c) Mintcheva, N.; Tanabe, M.; Osakada, K. *Organometallics* **2006**, *25*, 3776–3783.

(7) (a) Bennett, M. A.; Robertson, G. B.; Whimp, P. O.; Yoshida, T. *J. Am. Chem. Soc.* **1973**, *95*, 3028–3030. (b) Bennett, M. A.; Yoshida, T. *J. Am. Chem. Soc.* **1978**, *100*, 1750–1759. (c) Yoshida, T.; Okano, T.; Otsuka, S. *J. Chem. Soc., Dalton Trans.* **1976**, 993–999. (d) Bryndza, H. E.; Calabrese, J. C.; Wreford, S. S. *Organometallics* **1984**, *3*, 1603–1604. (e) Bryndza, H. E. *Organometallics* **1985**, *4*, 1686–1687. (f) Bryndza, H. E.; Tam, W. *Chem. Rev.* **1988**, *88*, 1163–1188.

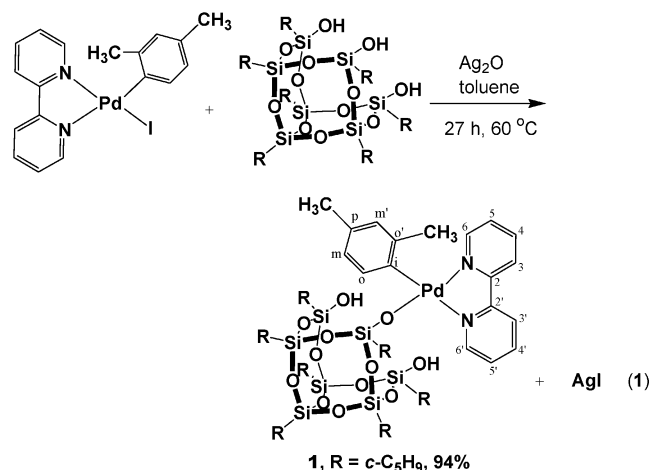
(8) (a) Kim, Y.-J.; Osakada, K.; Takenaka, A.; Yamamoto, A. *J. Am. Chem. Soc.* **1990**, *112*, 1096–1104. (b) Kim, Y.-J.; Choi, J.-C.; Osakada, K. *J. Organomet. Chem.* **1995**, *491*, 97–102. (c) Kapteijn, G. M.; Dervisi, A.; Grove, D. M.; Kooijman, H.; Lakin, M. T.; Spek, A. L.; van Koten, G. *J. Am. Chem. Soc.* **1995**, *117*, 10939–10949. (d) Kapteijn, G. M.; Dervisi, A.; Verhoef, M. J.; Frederik, M. A.; van den Broek, H.; Grove, D. M.; van Koten, G. *J. Organomet. Chem.* **1996**, *517*, 123–131. (e) Mann, G.; Hartwig, J. F. *J. Am. Chem. Soc.* **1996**, *118*, 13109–13110.

(9) (a) Bugno, C. D.; Pasquali, M.; Leoni, P.; Sabatino, P.; Braga, D. *Inorg. Chem.* **1989**, *28*, 1390–1394. (b) Alsters, P. L.; Baesjou, P. J.; Janssen, M. D.; Kooijman, H.; Sicherer-Roetman, A.; Spek, A. L.; van Koten, G. *Organometallics* **1992**, *11*, 4124–4135. (c) Kapteijn, G. M.; Grove, D. M.; Kooijman, H.; Smeets, W. J. J.; Spek, A. L.; van Koten, G. *Inorg. Chem.* **1996**, *35*, 526–533. (d) Kapteijn, G. M.; Meijer, M. D.; Grove, D. M.; Veldman, N.; Spek, A. L.; van Koten, G. *Inorg. Chim. Acta* **1997**, *264*, 211–217. (e) Kim, Y.-J.; Lee, J.-Y.; Osakada, K. *J. Organomet. Chem.* **1998**, *558*, 41–49. (f) Liu, X.; Renard, S. L.; Kilner, C. A.; Halcrow, M. A. *Inorg. Chem. Commun.* **2003**, *6*, 598–603.

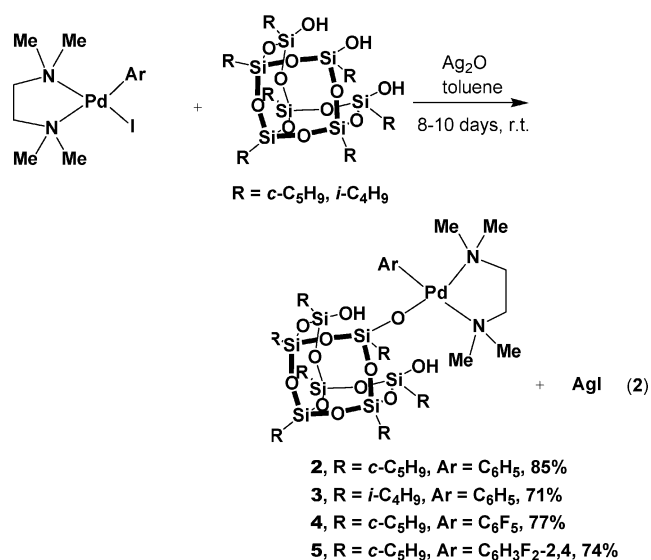
characterization, and dynamic behavior in solution of arylpalladium silsesquioxane complexes having chelating N-donor ligands.

Results and Discussion

The reaction of the incompletely condensed silsesquioxane ($c\text{-C}_5\text{H}_9$)₇Si₇O₉(OH)₃ with [Pd(C₆H₃Me₂-2,4)(I)(bpy)] in the presence of Ag₂O yielded a Pd complex with a monodentate-coordinated silsesquioxanate ligand, [Pd(C₆H₃Me₂-2,4){($c\text{-C}_5\text{H}_9$)₇Si₇O₁₀(OH)₂}(bpy)] (**1**), as shown in eq 1. Aryl(iodo)-



palladium complexes, [Pd(Ar)(I)(tmeda)] (Ar = C₆H₅, C₆F₅, C₆H₃F₂-2,4; tmeda = *N,N,N',N'*-tetramethylethylenediamine), also reacted with the silsesquioxanes R₇Si₇O₉(OH)₃ (R = $c\text{-C}_5\text{H}_9$, $i\text{-C}_4\text{H}_9$) at room temperature to produce complexes with a silsesquioxanate ligand, [Pd(Ar){R₇Si₇O₁₀(OH)₂}(tmeda)] (**2**, Ar = C₆H₅, R = $c\text{-C}_5\text{H}_9$; **3**, Ar = C₆H₅, R = $i\text{-C}_4\text{H}_9$; **4**, Ar = C₆F₅, R = $c\text{-C}_5\text{H}_9$; **5**, Ar = C₆H₃F₂-2,4, R = $c\text{-C}_5\text{H}_9$), as shown in eq 2. The reaction requires more time than the preparation



of *trans*-[Pt{R₇O₁₀Si₇(OH)₂}(Ph)(PET₃)₂] (R = $c\text{-C}_5\text{H}_9$, $i\text{-C}_4\text{H}_9$) (1–3 days).^{6c}

(10) (a) Fukuoka, A.; Sato, A.; Mizuho, Y.; Hirano, M.; Komiyama, S. *Chem. Lett.* **1994**, 1641–1644. (b) Fukuoka, A.; Sato, A.; Kodama, K.; Hirano, M.; Komiyama, S. *Inorg. Chim. Acta* **1999**, *294*, 266–274.

(11) Ruiz, J.; Vicente, C.; Rodríguez, V.; Cutillas, N.; López, G.; de Arellano, C. R. *J. Organomet. Chem.* **2004**, *689*, 1872–1875.

(12) Mintcheva, N.; Nishihara, Y.; Mori, A.; Osakada, K. *J. Organomet. Chem.* **2001**, *629*, 61–67.

Complexes **2** and **3** in toluene solutions decomposed upon heating at 60 °C, while the bpy-coordinated complex **1** was stable at that temperature. The higher stability of **1** as compared to that of **2** or **3** in solution may be ascribed to stable coordination of the bpy ligand compared with that of tmeda.

Complexes **1–5** were isolated as analytically pure solids and were characterized by ¹H, ¹³C{¹H}, ¹⁹F{¹H}, and ²⁹Si{¹H} NMR spectroscopy and/or X-ray crystallography. Figure 1 displays the molecular structure of **4**, as determined by X-ray crystallography. Selected bond lengths (Å) and angles (deg) are summarized in Table 1. The square-planar Pd(II) center is bonded to the chelating diamine ligand, a C₆F₅ group, and an O atom from a silanol site of the silsesquioxane. The Pd–O bond length (2.000(2) Å) is within the range of the bonds reported for aryloxo–palladium complexes (1.979–2.129 Å)^{9b–f} and alkoxo–palladium complexes (2.020–2.134 Å)^{8a,c} and is slightly longer than that in the siloxopalladium complex [Pd-(C₆F₅)(OSiPh₃)(tmeda)] (1.986(3) Å),¹¹ which may be ascribed to the high degree of electron-withdrawing character of the silsesquioxanate ligand compared with that of the OSiPh₃ ligand.^{2a} Pt complexes with silsesquioxanate or silanolate and phenyl ligands at *trans* positions, *trans*-[Pt{R₇O₁₀Si₇(OH)₂}(Ph)(PET₃)₂] (R = $c\text{-C}_5\text{H}_9$, $i\text{-C}_4\text{H}_9$) (Pt–O = 2.129(3), 2.113(2) Å)^{6c} and *trans*-[Pt{OSiMe₂(C₆H₄CF₃-4)}(Ph)(PPh₃)₂] (Pt–O = 2.091(4) Å),¹² contain a Pt–O bond that is longer than the Pd–O bond of **4**, partly because of the *trans* influence of the phenyl ligands in the complexes being greater than that of the chelating tmeda ligand. The Pd–N and Pd–C bond lengths of **4** are similar to those reported for [Pd(C₆F₅)(OSiPh₃)(tmeda)]¹¹ and [Pd(Me)(OR)(tmeda)] (R = alkyl).^{8b} The fact that the Pd–N1 distance (2.133(2) Å) is longer than the Pd–N2 distance (2.066(2) Å) in **4** suggests that the *trans* influence of the C₆F₅ group is greater than that of the silsesquioxanate ligand. The Pd–O–Si angle (133.0(1)°) is similar to those for the reported platinum silsesquioxane complexes (134.6(2) and 130.2(2)°)^{6c} and the siloxopalladium complex [Pd(C₆F₅)(OSiPh₃)(tmeda)] (137.9(2)°).¹¹

The crystal structure of **4** shows two intramolecular hydrogen bonds (O11–H1···O1 and O12–H2···O11) similarly to silsesquioxanate complexes containing platinum^{6c} or iron.¹³ The coordinated oxygen (O1) and an OH group (O11–H1) form a strong hydrogen bond (O1···O11 = 2.612(2) Å, O11–H1···O1 = 169(4)°), and the O···O distance is within the range of strong O–H···O hydrogen bonds (2.50–2.65 Å).¹⁴ The other hydrogen bond (O12–H2···O11) has an O···O distance (O11···O12 = 2.772(3) Å) longer than O1···O11 and an O12–H2···O11 angle (159(6)°) smaller than O11–H1···O1. As a result, the O12–H2···O11 hydrogen bond between the OH groups is weaker than the O11–H1···O1 hydrogen bond between the OH group and the coordinated O atom. Fluoroalkoxide and aryloxo ligands bonded to Pt and Pd were reported to form adducts having O–H···O hydrogen bonds between the alcohol or phenol and the coordinated oxygen.^{8a–c,9b,c,e} The O···O distances (2.56–2.66 Å) of the complexes indicate strong or medium hydrogen bonds. The crystallographic data of **4** show that the C₆F₅ group is almost perpendicular to the coordination plane, similarly to many other aryl complexes of d⁸ transition metals with a square-planar configuration. The O12···F1 distance (3.062(3) Å) is shorter than the sum of the van der Waals radii (3.88 Å)¹⁵ and is slightly

(13) Liu, F.; John, K. D.; Scott, B. L.; Baker, R. T.; Ott, K. C.; Tumas, W. *Angew. Chem., Int. Ed.* **2000**, *39*, 3127–3130.

(14) Gilli, P.; Bertolasi, V.; Ferretti, V.; Gilli, G. *J. Am. Chem. Soc.* **1994**, *116*, 909–915.

(15) Bondi, A. *J. Phys. Chem.* **1964**, *68*, 441–451.

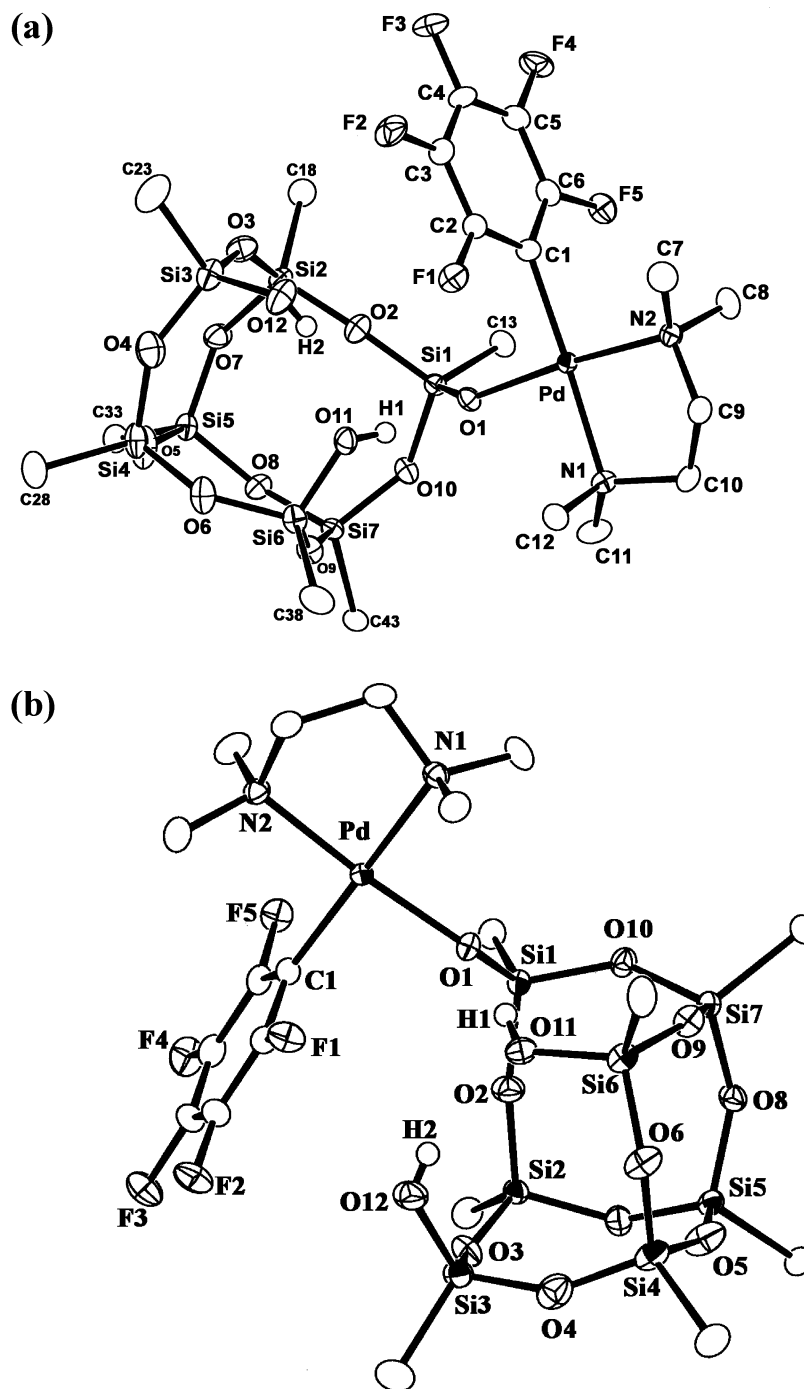


Figure 1. ORTEP drawing of **4** with ellipsoids at the 50% probability level. Hydrogen atoms, except OH hydrogens, and cyclopentyl substituents attached to Si atoms are omitted for simplicity.

Table 1. Selected Bond Distances (Å) and Angles (deg) of **4**

Pd–O1	2.000(2)	Si1–O1	1.606(2)
Pd–N1	2.133(2)	O1···O11	2.612(2)
Pd–N2	2.066(2)	O11···O12	2.772(3)
Pd–C1	2.003(3)		
O1–Pd–N1	89.75(9)	C1–Pd–N1	174.62(9)
O1–Pd–C1	90.8(1)	Pd–O1–Si1	133.0(1)
N1–Pd–N2	85.5(1)	O11–H1···O1	169(4)
N2–Pd–C1	93.9(1)	O12–H2···O11	159(6)
O1–Pd–N2	175.23(9)		

longer than the distances of the O–H···F hydrogen bonds reported (O···F < 2.97 Å).¹⁶ This molecule conformation having close contact between the F and O atoms (Figure 1b) suggests the presence of a weak interaction between the OH group and F atom, although competing O12–H2···O11 hydrogen bond

formation is more significant and results in a detectable electron density peak due to the H2 atom between O11 and O12 atoms rather than between the O12 and F1 atoms in the final *D* map.

The IR and ²⁹Si{¹H} and ¹³C{¹H} NMR spectra of **1–5** showed the coordination of the silsesquioxanate ligand to the Pd center. The IR spectra of **1–5** show a broad band from 3200 to 3350 cm⁻¹ due to the ν_{O–H} vibration of the hydroxy group engaged in O–H···O hydrogen bonding. The peaks at 731, 733, 735, 730, and 730 cm⁻¹, observed for **1–5**, respectively, are

(16) (a) Howard, J. A. K.; Hoy, V. J.; O'Hagan, D.; Smith, G. T. *Tetrahedron* **1996**, *52*, 12613–12622. (b) Wiechert, D.; Mootz, D.; Dahlems, T. *J. Am. Chem. Soc.* **1997**, *119*, 12665–12666. (c) Barbarich, T. J.; Rithner, C. D.; Miller, S. M.; Anderson, O. P.; Strauss, S. H. *J. Am. Chem. Soc.* **1999**, *121*, 4280–4281. (d) Li, H.; Lee, G.-H.; Peng, S.-M. *Inorg. Chem. Commun.* **2003**, *6*, 1–4.

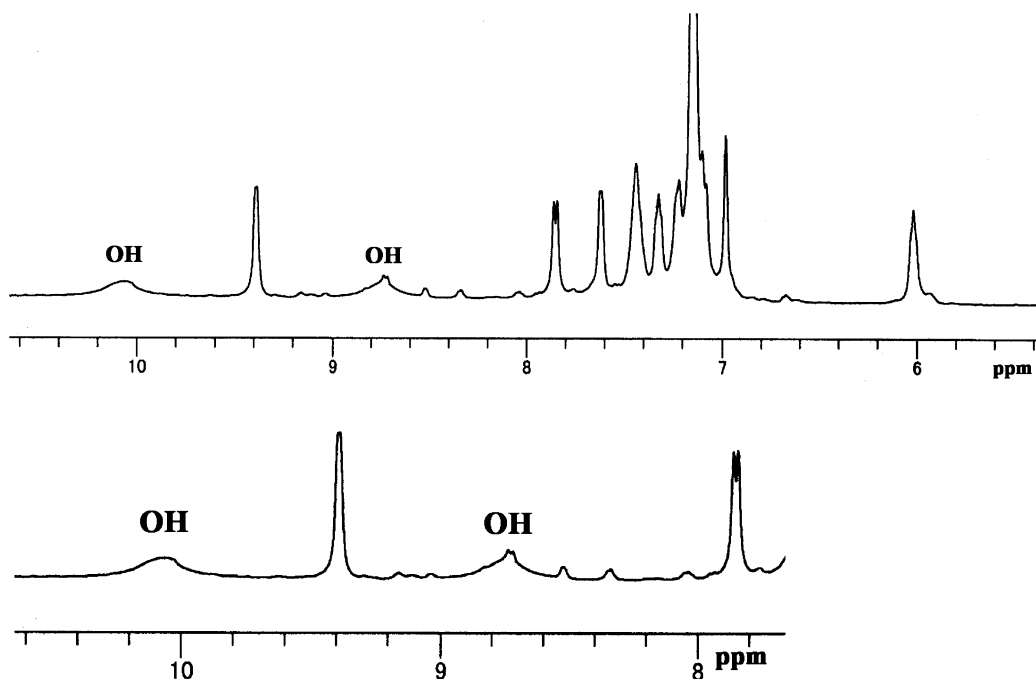
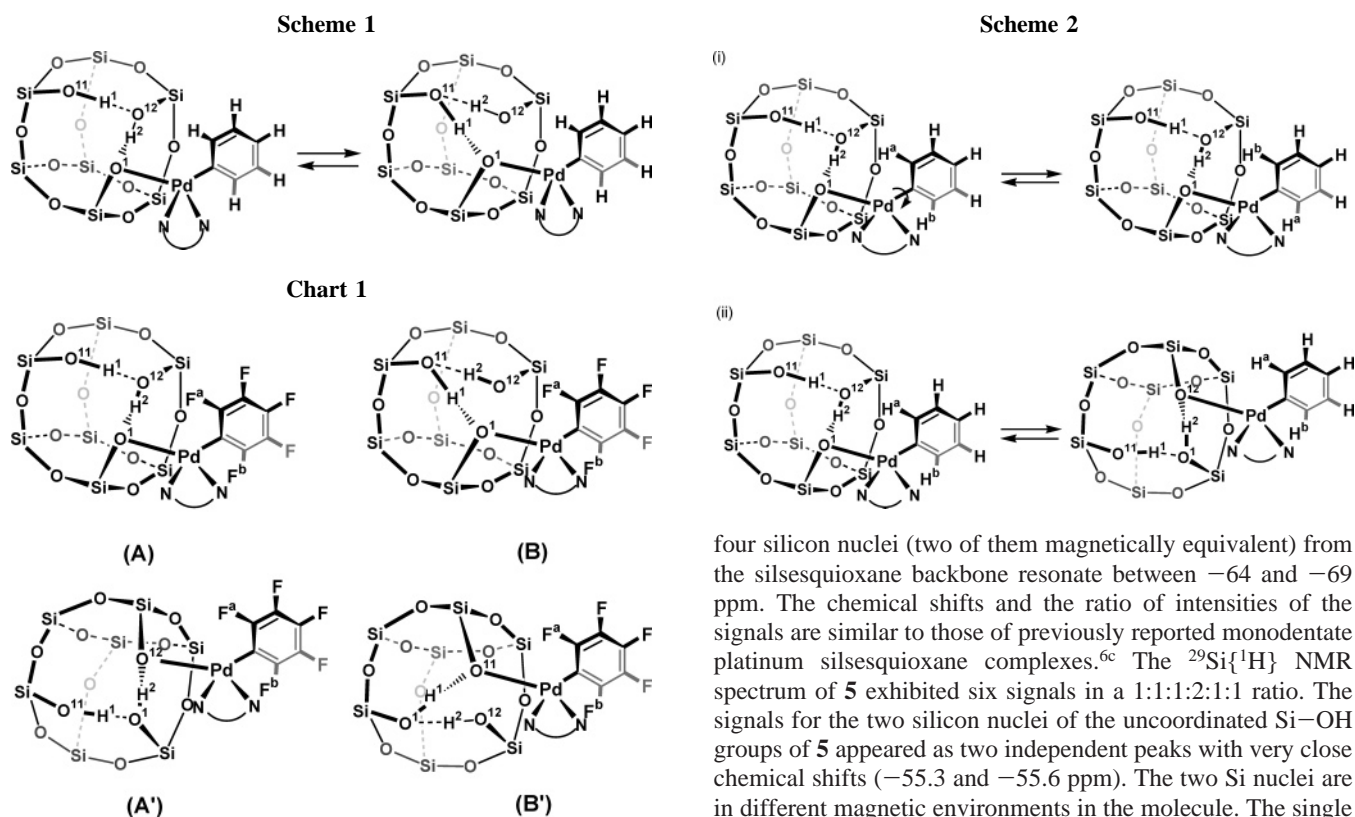


Figure 2. ^1H NMR spectra of **1** at room temperature in C_6D_6 .



assigned to the $\nu_{\text{Si-O}}$ vibrations of coordinated silanol groups and are in agreement with the IR data of reported monodentate-coordinated silsesquioxanates.^{6c}

Complex **1** exhibits seven $^{29}\text{Si}\{^1\text{H}\}$ NMR peaks for each of the ^{29}Si nuclei of the molecule. The $^{29}\text{Si}\{^1\text{H}\}$ NMR spectra of **2–4** consist of five signals in a 1:2:1:1:2 ratio, indicating the apparent C_m local symmetry of the silsesquioxanate ligand. The signal for two magnetically equivalent SiOH silicon nuclei and the signal for the silicon nucleus bonded to the coordinated oxygen appeared in the range from -55 to -58 ppm. The other

four silicon nuclei (two of them magnetically equivalent) from the silsesquioxane backbone resonate between -64 and -69 ppm. The chemical shifts and the ratio of intensities of the signals are similar to those of previously reported monodentate platinum silsesquioxane complexes.^{6c} The $^{29}\text{Si}\{^1\text{H}\}$ NMR spectrum of **5** exhibited six signals in a 1:1:1:2:1:1 ratio. The signals for the two silicon nuclei of the uncoordinated Si-OH groups of **5** appeared as two independent peaks with very close chemical shifts (-55.3 and -55.6 ppm). The two Si nuclei are in different magnetic environments in the molecule. The single peak for the two Si nuclei found for **2–4** is ascribed to the agreement of peak positions or to the dynamic behavior of the molecule in solution (vide infra).

The $^{13}\text{C}\{^1\text{H}\}$ NMR spectrum of **1** shows seven signals corresponding to the CH carbon atoms of cyclopentyl substituents, which is in agreement with the $^{29}\text{Si}\{^1\text{H}\}$ NMR spectral results. The $^{13}\text{C}\{^1\text{H}\}$ NMR spectra of **2–4** exhibit five signals for the methyne carbons of C_5H_9 groups (for **2** and **4**) and the CH_2 carbon atoms of isobutyl substituents of **3**, in a 1:1:2:2:1 peak ratio in the range 22.4–26.4 ppm. One of the signals is at downfield positions (25.6 (**2**), 26.4 (**3**), 25.2 ppm (**4**)) compared

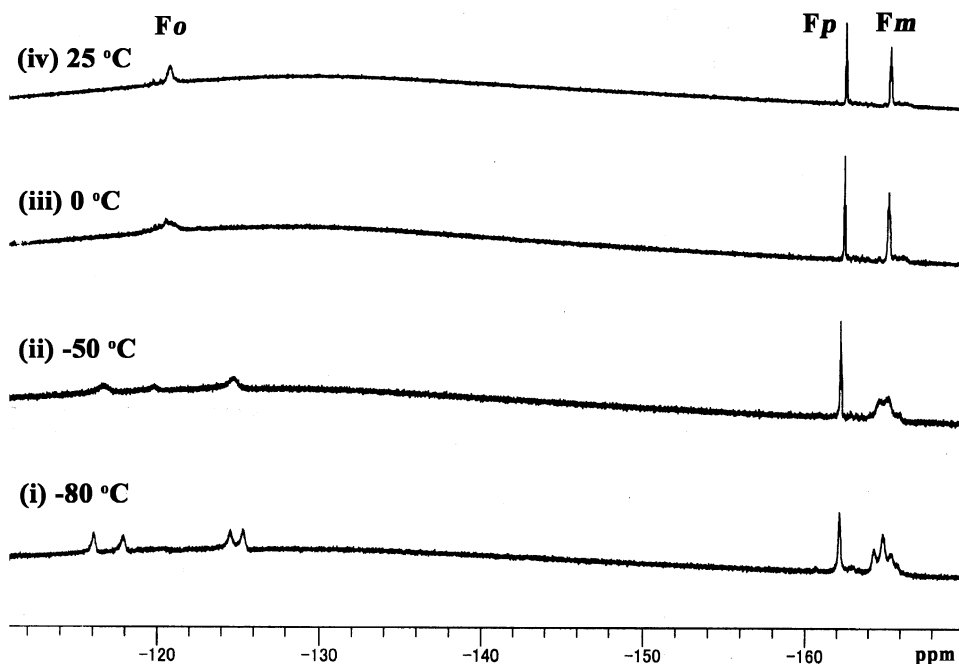


Figure 3. Variable-temperature $^{19}\text{F}\{^1\text{H}\}$ NMR spectra of **4** in toluene- d_8 .

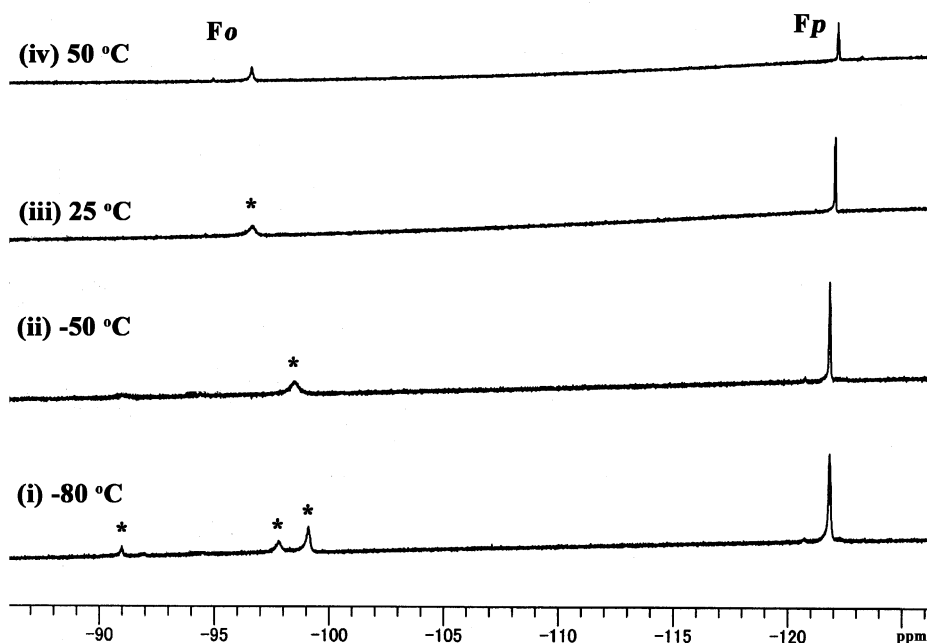


Figure 4. Variable-temperature $^{19}\text{F}\{^1\text{H}\}$ NMR spectra of **5** in toluene- d_8 .

with the other signals and is assigned to the carbon of an alkyl group bonded to the Si atom of the Si–O–Pd group. The ratios of the peaks are in agreement with the ratio of ^{29}Si NMR signals. The chemical shifts of the aromatic carbon atoms of **2–4** are in good agreement with those reported for $[\text{PdI}(\text{C}_6\text{H}_5)(\text{tmeda})]$ and $[\text{PdI}(\text{C}_6\text{F}_5)(\text{tmeda})]$.¹⁷ Two doublets of **4** with a coupling constant of 230–240 Hz were observed and assigned to C_o and C_m of the C_6F_5 group. The assignment of ^{13}C NMR signals for the difluorophenyl ligand of **5** is based on a C–H COSY diagram and the C–F coupling constants. The signals for the C–F carbons appear as a doublet of doublets at 164.63 and

161.05 ppm with the following coupling constants: $J_{\text{CF}} = 230$ Hz, $^3J_{\text{CF}} = 11$ Hz and $J_{\text{CF}} = 240$ Hz, $^3J_{\text{CF}} = 12$ Hz. The signal observed at 138.47 ppm due to the ortho CH carbon atom shows coupling with two F nuclei ($^3J_{\text{CF}} = 19$ Hz, $^3J_{\text{CF}} = 7.4$ Hz). A doublet of doublets at 101.45 ppm ($^2J_{\text{CF}} = 33$ Hz, $^2J_{\text{CF}} = 24$ Hz) and an apparent triplet due to similar ^{13}C – ^{19}F coupling constants (122.73 ppm, $^2J_{\text{CF}} = 40$ Hz) are attributed to the two CH carbon atoms at the meta position.

The ^1H NMR spectrum of **1** in C_6D_6 at room temperature shows two signals at 2.71 and 2.38 ppm for ortho or para CH_3 hydrogens. As shown in Figure 2, the OH hydrogen signals are observed as two broad signals at 10.1 and 8.7 ppm. They are assigned to $\text{O}-\text{H}\cdots\text{OPd}$ hydrogen and $\text{O}-\text{H}\cdots\text{OH}$ hydrogen,

(17) Martinez-Viviente, E.; Pregosin, P. S.; Tschoerner, M. *Magn. Reson. Chem.* **2000**, *38*, 23–28.

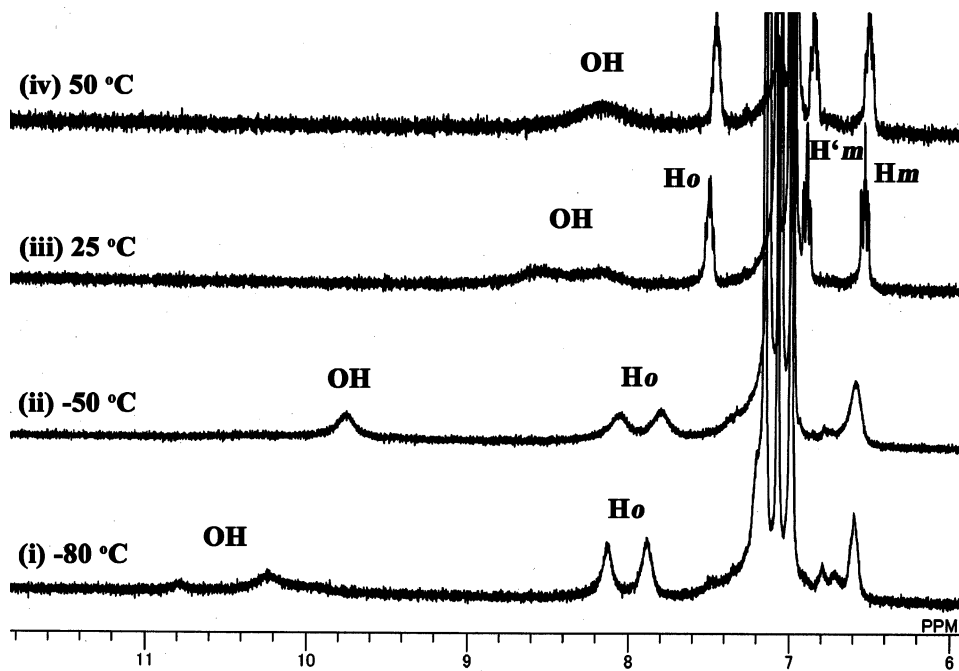
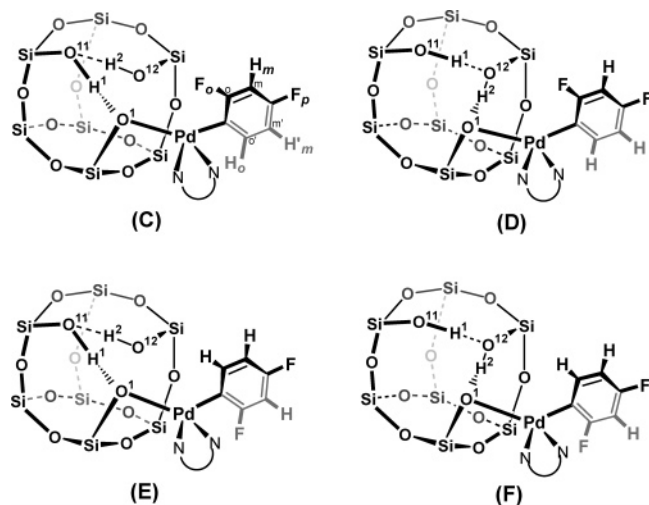


Figure 5. Variable-temperature ^1H NMR spectra of **5** in toluene- d_8 .

Chart 2



respectively, because the former group contains a stronger $\text{O}-\text{H}\cdots\text{O}$ hydrogen bond than the latter. The low magnetic field positions of the peaks indicate the formation of $\text{O}-\text{H}\cdots\text{O}$ hydrogen bonding in solution. NMR and calorimetric studies of Pd, Pt, and Rh complexes with fluoroalkoxide or aryloxide ligands and associated alcohols or phenols through $\text{O}-\text{H}\cdots\text{O}$ hydrogen bonds^{8a-c,9b,c,e,18} showed large association constants in solution. The formation constants of $[\text{Rh}(\text{OAr})(\text{OHAr})(\text{PMe}_3)_3]$ are comparable with those between proton donors and anionic electron-pair donors.¹⁸

The ^1H NMR spectra of **2–5** in toluene- d_8 exhibit a single broad signal of OH hydrogens of silsesquioxane in the range of 7.8–9.0 ppm at room temperature, similarly to those of the Pt and Sn complexes with incompletely condensed silsesquioxanate ligands.^{6c,19} The two OH hydrogens of **2** and **3** under different circumstances are observed as a single broad signal owing to rapid exchange, as shown in Scheme 1.

The activation of the $\text{O1}\cdots\text{H2}$ and $\text{O12}\cdots\text{H1}$ hydrogen bonds of the structure on the left, accompanied by the formation of new hydrogen bonds, $\text{O1}\cdots\text{H1}$ and $\text{O11}\cdots\text{H2}$, leads to the structure shown on the right. This concerted process of **2** and **3** takes place more rapidly than the NMR time scale, although complex **1** undergoes this switching of hydrogen bonds more slowly and exhibits two ^1H NMR signals for the OH hydrogens at room temperature.

We reported that $\text{trans}-[\text{Pt}\{\text{R}_7\text{O}_{10}\text{Si}_7(\text{OH})_2\}(\text{Ph})(\text{PEt}_3)_2]$ ($\text{R} = \text{c-C}_5\text{H}_9, \text{i-C}_4\text{H}_9$) exhibits two signals for ortho hydrogens of the phenyl ligand at $-50\text{ }^\circ\text{C}$ and that they undergo coalescence with an increase in temperature.^{6c} Two processes are able to account for the dynamic behavior of the molecule. One involves the rotation of the Pd–C bond, shown in part i of Scheme 2, even though the concurrent activation of the Pd–O and O–H bonds and the formation of new Pd–O and O–H bonds (part ii of Scheme 2) would also result in appearance of a single OH hydrogen peak. The latter process was proposed to account for the temperature-dependent NMR spectra of not only $\text{trans}-[\text{Pt}\{\text{R}_7\text{O}_{10}\text{Si}_7(\text{OH})_2\}(\text{Ph})(\text{PEt}_3)_2]$ ^{6c} but also the Pd and Pt alkoxide or aryloxide complexes with alcohols (or phenols) associated via $\text{O}-\text{H}\cdots\text{O}$ hydrogen bonds.

Variable-temperature ^1H and $^{19}\text{F}\{^1\text{H}\}$ NMR studies of **4** and **5** in toluene- d_8 revealed the unique dynamic behavior of the molecules. Figure 3 shows the temperature-dependent $^{19}\text{F}\{^1\text{H}\}$ NMR spectra of **4**. The spectrum at $-80\text{ }^\circ\text{C}$ exhibits two pairs of signals for the ortho fluorine atoms of the C_6F_5 ligand. The pairs of signals are assigned to two conformational isomers, **A** and **B**, in Chart 1. Isomer **B** corresponds to the crystallographically determined structure (Figure 1) that contains hydrogen bonds $\text{O11}-\text{H1}\cdots\text{O1}$ and $\text{O12}-\text{H2}\cdots\text{O11}$ and shows close contact between O12 and the F_a atom. It shows a pair of $^{19}\text{F}\{^1\text{H}\}$ NMR signals due to a perpendicular relationship between the aryl plane and the coordination plane.

Structure **A** has another combination of O and H atoms forming hydrogen bonds within the silsesquioxanate ligand ($\text{O11}-\text{H1}\cdots\text{O12}$ and $\text{O12}-\text{H2}\cdots\text{O1}$), and it also gives rise to a pair of $^{19}\text{F}\{^1\text{H}\}$ NMR signals for ortho F nuclei. Although the two isomers are distinguishable by $^{19}\text{F}\{^1\text{H}\}$ NMR at low

(18) Duchateau, R.; Dijkstra, T. W.; Severn, J. R.; van Santen, R. A.; Korobkov, I. V. *Dalton Trans.* **2004**, 2677–2682.

(19) Kegley, S. E.; Schaverien, C. J.; Freudenberger, J. H.; Bergman, R. G.; Nolan, S. P.; Hoff, C. D. *J. Am. Chem. Soc.* **1987**, *109*, 6563–6565.

temperatures, at $-50\text{ }^{\circ}\text{C}$ the NMR signals coalesce to give rise to two signals for the ortho fluorine nuclei. This indicates that a mutual exchange between **A** and **B** is taking place on the NMR time scale, which is similar to the exchange shown for **2** in Scheme 1. The structural change involves the switching of hydrogen bonds and may accompany a change in the conformation induced by the rotation of the Pd–O bond to a limited extent. The spectrum at $0\text{ }^{\circ}\text{C}$ shows a broad signal for the ortho fluorine nuclei, suggesting that another dynamic behavior occurs at this temperature and renders all fluorine atoms at the ortho position equivalent. Mutual exchange between **A** and **A'** and that between **B** and **B'** (Chart 1) account for the NMR spectra change. They correspond to the dynamic behavior of **2** in Scheme 2; either the rotation of the Pd–C bond or the metathesis-type switching of the Pd–O and O–H bonds is able to make the two ortho positions of the aryl ligand of the complexes equivalent. The $^{19}\text{F}\{^1\text{H}\}$ NMR spectrum of **4** at $-80\text{ }^{\circ}\text{C}$ indicated the presence of two isomers, **A** and **B**, although the ^1H NMR spectra of **2** at low temperatures were not helpful in distinguishing the corresponding isomers.

The $^{19}\text{F}\{^1\text{H}\}$ NMR spectra of **5** at different temperatures are shown in Figure 4. The spectrum at $25\text{ }^{\circ}\text{C}$ shows two signals at -122.0 and -96.7 ppm, which are assigned to the fluorine nuclei at the para and ortho positions, respectively. The signal for the para fluorine nucleus is temperature-independent, whereas that for the ortho fluorine nucleus is temperature-dependent. Decreasing the temperature to $-80\text{ }^{\circ}\text{C}$ gives rise to three signals in a ratio of approximately 1:1:2 for ortho fluorine atoms. Figure 5 shows the VT ^1H NMR spectra of **5**. The ^1H NMR spectrum of **5** at $50\text{ }^{\circ}\text{C}$ (part iv in Figure 5) shows the displacement of three multiple signals (at 6.54, 6.90, and 7.50 ppm) for three nonequivalent hydrogens from the difluoro-substituted phenyl group. According to the C–H COSY diagram and F–H coupling constants in CDCl_3 solution, they are assigned to two nonequivalent H_m atoms (H_m and H'_m) and H_o , respectively. The signal for H_m (located between F_o and F_p) is temperature-independent, whereas the signal for H'_m overlaps with solvent peaks at low temperatures. The signal for H_o splits into two components at $-50\text{ }^{\circ}\text{C}$ (part ii in Figure 5).

Chart 2 depicts four possible conformational isomers of **5** existing in solution. Structures **C** and **D** have the ortho fluorine atom of the $\text{C}_6\text{H}_3\text{F}_2$ ligand and the OH groups of the silsesquioxane ligand on the same side of the coordination plane and have positions of O–H \cdots O hydrogen bonding that differ from each other, similarly to **A** and **B** in Chart 1. Structures **E** and **F** have the ortho fluorine atom and OH group on opposite side of the coordination plane. The coalescence of the NMR signals is due to dynamic processes involving a mutual conversion between **C** and **D** or **E** and **F** similarly to Scheme 1, and that between **C** and **E** or **D** and **F** similarly to Scheme 2. The $^{19}\text{F}\{^1\text{H}\}$ NMR signals at -91.0 and -97.8 ppm assigned to **C** and **D** appear at different positions, similarly to the corresponding fluorine atoms of **A** and **B**. Isomers **E** and **F** exhibit a single $^{19}\text{F}\{^1\text{H}\}$ NMR signal at -99.1 ppm. The ^1H NMR spectrum shows two signals for the ortho hydrogen, even at $-80\text{ }^{\circ}\text{C}$. It may be ascribed to a $^{19}\text{F}\{^1\text{H}\}$ NMR peak position (ca. 2500 Hz) that is much larger than and different from the ^1H NMR peak difference (ca. 500 Hz).

The ^1H NMR signals of OH hydrogens of **5** are more complicated than those of the OH hydrogen atoms of **2** and **4**. Two weak and broad signals at 8.18 and 8.55 ppm are observed at $25\text{ }^{\circ}\text{C}$. Increasing the temperature leads to one broad signal at 8.2 ppm, whereas the spectra at low temperatures show one

or two signals depending on the temperature (-50 , $-80\text{ }^{\circ}\text{C}$). This result may be ascribed to the presence of isomers in Chart 2.

Conclusion

The first crystal structure of palladium silsesquioxane containing a monodentate O-coordinated silsesquioxane ligand was obtained. Arylpalladium silsesquioxanate complexes with a diamine ligand and three types of aryl groups were synthesized and characterized. The dynamic behavior of phenylpalladium silsesquioxane complexes (**2** and **3**) in solution involves the rotation of a Ph ring around the Pd–C bond and the rapid exchange of H atoms between both O–H \cdots O hydrogen bonds. Fluoro-substituted phenylpalladium complexes (**4** and **5**) revealed the presence of conformational isomers and their mutual exchange on the NMR time scale.

Experimental Section

General Procedures. All manipulations of the complexes were carried out using standard Schlenk techniques under an argon or nitrogen atmosphere. Toluene and hexane for the reactions were dried using a Grubbs type solvent system stored under nitrogen.²⁰ Aryliodopalladium(II) complexes, $[\text{Pd}(\text{Ar})(\text{I})(\text{tmeda})]$ (Ar = C_6H_5 , $\text{C}_6\text{H}_3\text{F}_2$ -2,4, C_6F_5 ; tmeda = *N,N,N',N'*-tetramethylethylenediamine), and $[\text{Pd}(\text{I})(\text{C}_6\text{H}_3\text{Me}_2$ -2,4)(bpy)] were prepared by oxidative addition of iodoarene to $\text{Pd}(\text{dba})_2$ (dba = dibenzylideneacetone)²¹ in the presence of tmeda (or bpy), as previously reported.^{22–24} The silsesquioxanes 1,3,5,7,9,11,14-heptacyclopentyltricyclo[7.3.3.1(5,-11)]heptasiloxane-*endo*-3,7,14-triol ($(\text{C}-\text{C}_5\text{H}_9)_7\text{Si}_7\text{O}_9(\text{OH})_3$) and 1,3,5,7,9,11,14-heptaisobutyltricyclo[7.3.3.1(5,11)]heptasiloxane-*endo*-3,7,14-triol ($(i-\text{C}_4\text{H}_9)_7\text{Si}_7\text{O}_9(\text{OH})_3$) are commercially available products of Aldrich Chemical Co. Ag_2O was purchased from Wako Pure Chemical Ind., Ltd. The reagents were used without any purification. ^1H , $^{13}\text{C}\{^1\text{H}\}$, $^{19}\text{F}\{^1\text{H}\}$, and $^{29}\text{Si}\{^1\text{H}\}$ NMR spectra were recorded on Varian Mercury 300 and JEOL EX-400 spectrometers. Chemical shifts of the signals in ^1H and $^{13}\text{C}\{^1\text{H}\}$ NMR spectra were adjusted to the residual peaks of the solvents used. Peak positions in the $^{29}\text{Si}\{^1\text{H}\}$ and $^{19}\text{F}\{^1\text{H}\}$ NMR spectra were referenced to external standard SiMe_4 in C_6D_6 (or CDCl_3) and CF_3COOH in toluene-*d*₈, respectively. IR absorption spectra were recorded on a Shimadzu FT/IR-8100 spectrometer. Elemental analyses were carried out with a LECO CHNS-932 or Yanaco MT-5 CHN autocorder. New complexes obtained undergo decomposition without melting upon heating. The temperature of starting decomposition (dec pt) is shown for each complex.

Preparation of $[\text{Pd}\{(\text{C}-\text{C}_5\text{H}_9)_7\text{Si}_7\text{O}_{10}(\text{OH})_2\}(\text{C}_6\text{H}_3\text{Me}_2$ -2,4)-(bpy)] (1**).** To a solution of $[\text{Pd}\{(\text{C}_6\text{H}_3\text{Me}_2$ -2,4)(bpy)] (136 mg, 0.30 mmol) in toluene (15 mL) were added $(\text{C}-\text{C}_5\text{H}_9)_7\text{Si}_7\text{O}_9(\text{OH})_3$ (262 mg, 0.30 mmol) and Ag_2O (84 mg, 0.36 mmol). The reaction mixture was heated at $60\text{ }^{\circ}\text{C}$ for 27 h and then filtered through Celite. The solvent was evaporated under reduced pressure, and the crude product was washed with hexane (3×5 mL) to afford **1** as a yellow solid (380 mg, 94%). Anal. Calcd for $\text{C}_{53}\text{H}_{83}\text{N}_2\text{O}_{12}$ -PdSi₇: C, 51.24; H, 6.65; N, 2.26. Found: C, 50.93; H, 6.55; N, 2.20. Dec pt: $178\text{ }^{\circ}\text{C}$. ^1H NMR (300 MHz, CDCl_3 , room

(20) Pangborn, A. B.; Giardello, M. A.; Grubbs, R. H.; Rosen, R. K.; Timmers, F. J. *Organometallics* **1996**, *15*, 1518–1520.

(21) Ukai, T.; Kawazura, H.; Ishii, Y.; Bonnet, J. J.; Ibers, J. A. *J. Organomet. Chem.* **1974**, *65*, 253–266.

(22) Markies, B. A.; Cauty, A. J.; de Graaf, W.; Boersma, J.; Janssen, M. D.; Hogerheide, M. P.; Smeets, W. J. J.; Spek, A. L.; van Koten, G. *J. Organomet. Chem.* **1994**, *482*, 191–199.

(23) Hughes, R. P.; Ward, A. J.; Golen, J. A.; Incarvito, C. D.; Rheingold, A. L.; Zakharov, L. N. *Dalton Trans.* **2004**, 2720–2727.

(24) Yagyu, T.; Osakada, K.; Brookhart, M. *Organometallics* **2000**, *19*, 2125–2129.

Table 2. Crystallographic Data and Details of Refinement of 4

empirical formula	C ₄₇ H ₈₁ F ₅ N ₂ O ₁₂ PdSi ₇
formula wt	1264.15
cryst color	pale yellow
cryst dimens (mm)	0.70 × 0.30 × 0.15
cryst syst	monoclinic
space group	<i>P</i> 2 ₁ / <i>n</i> (No. 14)
<i>a</i> (Å)	13.260(2)
<i>b</i> (Å)	24.742(3)
<i>c</i> (Å)	18.376(2)
β (deg)	102.788(1)
<i>V</i> (Å ³)	5879(1)
<i>Z</i>	4
calcd density (g cm ⁻³)	1.428
<i>F</i> (000)	2648
μ (cm ⁻¹)	5.312
no. of rflns measd	43 230
no. of unique rflns	13 384
<i>R</i> _{int}	0.031
no. of variables	754
<i>R</i> 1 (<i>I</i> > 2.00 σ (<i>I</i>))	0.0444
w <i>R</i> 2 (<i>I</i> > 2.00 σ (<i>I</i>))	0.1288
goodness of fit	0.994

temperature): δ 0.8–1.2 (m, 7H, CH pentyl), 1.2–2.0 (m, 56H, CH₂ pentyl), 2.27 (s, 3H, CH₃), 2.47 (s, 3H, CH₃), 6.69 (d, 1H, PdC₆H₄ meta, *J*_{HH} = 7.8 Hz), 6.74 (s, 1H, PdC₆H₄ meta'), 7.01 (t, 1H, H_{5'} bpy, *J*_{HH} = 6.6 Hz), 7.39 (d, 1H, PdC₆H₄ ortho, *J*_{HH} = 7.2 Hz), 7.43 (m, 1H, H₅ bpy), 7.55 (1H, OH), 7.73 (d, 1H, H_{6'} bpy, *J*_{HH} = 5.4 Hz), 7.82 (t, 1H, H₄ bpy, *J*_{HH} = 7.5 Hz), 8.01–8.23 (overlapped 3H, H_{3,3'} bpy and H_{4'} bpy), 9.11 (d, 1H, H₆ bpy, *J*_{HH} = 4.5 Hz), 9.6 (1H, OH). ¹H NMR (300 MHz, C₆D₆, room temperature): δ 1.1–1.4 (m, 7H, CH pentyl), 1.4–2.2 (m, 56H, CH₂ pentyl), 2.38 (s, 3H, CH₃), 2.71 (s, 3H, CH₃), 6.05 (t, 1H, H_{5'} bpy, *J*_{HH} = 6.3 Hz), 6.95 (s, 1H, PdC₆H₄ meta'), 7.08 (d, 1H, PdC₆H₄ meta, *J*_{HH} = 7.8 Hz), 7.22 (m, 3H, overlapped H₅ bpy and H_{3,3'} bpy), 7.49 (m, 2H, H_{4,4'} bpy), 7.76 (d, 1H, H_{6'} bpy, *J*_{HH} = 5.4 Hz), 7.83 (d, 1H, PdC₆H₄ ortho, *J*_{HH} = 7.8 Hz), 8.7 (1H, OH), 9.31 (dd, 1H, H₆ bpy, *J*_{HH} = 4.8, 1.8 Hz), 10.1 (1H, OH). ¹³C{¹H} NMR (100 MHz, C₆D₆, room temperature): δ 21.08 (CH₃), 23.11, 23.16, 23.31, 23.39, 23.79, 23.83, 24.24 (7C, CH pentyl), 25.10, 25.22 (CH₃), 27.59–29.45 (28C, CH₂ pentyl), 121.69 (C_{4'} bpy), 123.23 (C_{3'} bpy), 124.94 (PdC₆H₃ meta), 125.63 (C_{5'} bpy), 126.20 (C₅ bpy), 128.53 (C₃ bpy), 130.16 (PdC₆H₃ meta'), 132.88 (PdC₆H₃ para), 135.99 (C_{6'} bpy), 138.37 (PdC₆H₃ ortho), 138.86 (PdC₆H₃ ortho'), 140.06 (PdC₆H₃ ipso), 149.63 (C₆ bpy), 151.72 (C₄ bpy), 152.33 (C_{2'} bpy), 156.22 (C₂ bpy). The peak positions of H and C atoms were assigned using H–H COSY and C–H COSY diagrams. ²⁹Si{¹H} NMR (79 MHz, C₆D₆, 0.02 M Cr(acac)₃, room temperature): δ -54.83, -56.11, -56.71, -64.46, -64.76, -66.54, -67.58. IR data (KBr): 3300 (br w), 2950 (s), 2865 (s), 1599 (w), 1468 (w), 1447 (m), 1244 (m), 1109 (vs), 900 (m), 764 (m), 731 (w), 502 (m) cm⁻¹.

Preparation of [Pd{(c-C₅H₉)₇Si₇O₁₀(OH)₂}(C₆H₅)(tmeda)] (2).

To a solution of [PdI(C₆H₅)(tmeda)] (64 mg, 0.15 mmol) in toluene (8 mL) were added (c-C₅H₉)₇Si₇O₉(OH)₃ (131 mg, 0.15 mmol) and Ag₂O (42 mg, 0.18 mmol). The reaction mixture was stirred at room temperature for 8 days. The gray suspension was passed through a Celite pad, and the Celite was washed with 4 mL of toluene. The solvent was evaporated under reduced pressure. Then 1 mL of hexane was added and the solution was kept at -20 °C to give **2** as a yellow solid (150 mg, 85%). Anal. Calcd for C₄₇H₈₆N₂O₁₂PdSi₇: C, 48.08; H, 7.38; N, 2.39. Found: C, 47.87; H, 7.16; N, 2.46. Dec pt: 159 °C. ¹H NMR (300 MHz, CDCl₃, room temperature): δ 0.71 (m, 1H, CH pentyl), 0.98 (m, 6H, CH pentyl), 1.3–2.0 (m, 56H, CH₂ pentyl), 2.43 (s, 6H, N(CH₃)), 2.50 (m, 2H, NCH₂), 2.61 (s, 6H, N(CH₃)), 2.65 (m, 2H, NCH₂), 6.80–6.90 (m, 3H, PdC₆H₅ meta and para), 7.28 (d, 2H, PdC₆H₅ ortho), 8.6 (br, 2H, OH). ¹³C{¹H} NMR (100 MHz, CDCl₃, room temperature): δ 22.54, 22.63, 22.67, 23.08, 25.64 (1:1:2:2:1, 7C,

CH pentyl), 27.06, 27.10, 27.14, 27.18, 27.31, 27.34, 27.39, 27.66, 27.68, 28.93 (28C, CH₂ pentyl), 47.54 (N(CH₃)₂), 51.39 (N(CH₃)₂), 57.84 (CH₂), 63.38 (CH₂), 122.67 (PdC₆H₅ para), 125.84 (PdC₆H₅ meta), 135.05 (PdC₆H₅ ortho), 148.65 (PdC₆H₅ ipso). ²⁹Si{¹H} NMR (79 MHz, C₆D₆, 0.02 M Cr(acac)₃, room temperature): δ -55.76, -56.57, -64.47, -64.95, -67.53 (1:2:1:1:2). IR data (KBr): 3200 (br, w), 2949 (s), 2865 (s), 1560 (w), 1474 (m), 1458 (w), 1246 (m), 1100 (vs), 930 (m), 878 (m), 804 (w), 763 (w), 733 (w), 698 (w), 502 (m) cm⁻¹.

Preparation of [Pd{(i-C₄H₉)₇Si₇O₁₀(OH)₂}(C₆H₅)(tmeda)] (3).

To a solution of [PdI(C₆H₅)(tmeda)] (64 mg, 0.15 mmol) in toluene (8 mL) were added (i-C₄H₉)₇Si₇O₉(OH)₃ (119 mg, 0.15 mmol) and Ag₂O (42 mg, 0.18 mmol). The reaction mixture was stirred at room temperature for 8 days. After filtration through Celite and removal of the solvent, the crude product was dissolved in 1 mL of hexane and kept at -20 °C for 2 days to afford a yellow solid (117 mg, 71%). Anal. Calcd for C₄₀H₈₆N₂O₁₂PdSi₇: C, 44.07; H, 7.95; N, 2.57. Found: C, 43.57; N, 2.62; H, 7.63. Dec pt: 126 °C. ¹H NMR (300 MHz, CDCl₃, room temperature): δ 0.26 (d, 4H, CH₂ iBu, *J*_{HH} = 6.9 Hz), 0.49 (d, 2H, CH₂ iBu, *J*_{HH} = 6.6 Hz), 0.55 (d, 2H, CH₂ iBu, *J*_{HH} = 6.9 Hz), 0.62 (d, 4H, CH₂ iBu, *J*_{HH} = 6.9 Hz), 0.71 (d, 2H, CH₂ iBu, *J*_{HH} = 6.9 Hz), 0.83 (d, 12H, CH₃ iBu, *J*_{HH} = 6.6 Hz), 0.88 (d, 6H, CH₃ iBu, *J*_{HH} = 6.6 Hz), 0.94 (d, 6H, CH₃ iBu, *J*_{HH} = 6.6 Hz), 0.99 (m, 18H, CH₃ iBu), 1.6 (m, 2H, CH iBu), 1.8 (m, 4H, CH iBu), 2.1 (m, 1H, CH iBu), 2.43 (s, 6H, N(CH₃)₂), 2.52 (m, 2H, NCH₂), 2.57 (s, 6H, N(CH₃)₂), 2.65 (m, 2H, NCH₂), 6.83–6.89 (m, 3H, PdC₆H₅ para and meta), 7.30 (d, 2H, PdC₆H₅ ortho, *J*_{HH} = 6.6 Hz), 8.8 (br, 2H, OH). ¹³C{¹H} NMR (100 MHz, CDCl₃, room temperature): δ 22.74, 22.87, 22.93, 23.35, 26.45 (1:1:2:2:1, 7C, CH₂ iBu), 23.81, 23.95, 23.97, 24.10, 24.87 (2:1:1:2:1, 7C, CH iBu), 25.64, 25.76, 25.80, 25.93, 26.01, 26.25 (2:2:2:3:3:2, 14C, CH₃ iBu), 47.38 (N(CH₃)₂), 51.31 (N(CH₃)₂), 57.70 (CH₂), 63.31 (CH₂), 122.80 (PdC₆H₅ para), 125.88 (PdC₆H₅ meta), 135.30 (PdC₆H₅ ortho), 148.76 (PdC₆H₅ ipso). The signals for CH, CH₂, and CH₃ carbon atoms of isobutyl substituents were assigned by the DEPT method. ²⁹Si{¹H} NMR (79 MHz, CDCl₃, 0.02 M Cr(acac)₃, room temperature): δ -56.98, -57.78, -66.54, -67.08, -69.17 (ratio 2:1:2:1:1). IR data (KBr): 3250 (br, w), 2953 (s), 2869 (s), 1566 (w), 1466 (m), 1458 (w), 1402 (w), 1366 (w), 1331 (w), 1229 (m), 1100 (vs), 959 (m), 907 (m), 853 (w), 804 (w), 770 (w), 735 (m), 698 (w), 484 (m) cm⁻¹.

Preparation of [Pd{(c-C₅H₉)₇Si₇O₁₀(OH)₂}(C₆F₅)(tmeda)] (4).

To a solution of [PdI(C₆F₅)(tmeda)] (54 mg, 0.10 mmol) in toluene (5 mL) were added (c-C₅H₉)₇Si₇O₉(OH)₃ (87 mg, 0.10 mmol) and Ag₂O (28 mg, 0.12 mmol). The reaction mixture was stirred at room temperature for 10 days, after that it was filtered through Celite. The solvent was evaporated and the product was recrystallized from hexane (1 mL) at -20 °C as pale yellow crystals suitable for X-ray crystallography (98 mg, 75%). Anal. Calcd for C₄₇H₈₁F₅N₂O₁₂PdSi₇: C, 44.65; N, 2.22; F, 7.51; H, 6.46. Found: C, 44.79; N, 2.20; F, 7.62; H, 6.32. Dec pt: 182 °C. ¹H NMR (400 MHz, C₇D₈, room temperature): δ 1.0–1.4 (m, 7H, CH pentyl), 1.4–2.0 (m, overlapped 56H, CH₂ pentyl and 4H, NCH₂), 1.66 (s, 6H, NCH₃), 2.36 (s, 6H, NCH₃), 7.8 (br, 2H, OH). ¹⁹F{¹H} NMR (376 MHz, C₇D₈, room temperature): δ -120.7 (br, 2F ortho), -162.5 (t, 1F para, *J*_{FF} = 20 Hz), -165.3 (m, 2F meta, *J*_{FF} = 20 Hz). ¹³C{¹H} NMR (100 MHz, CDCl₃, room temperature): δ 22.44, 22.54, 22.73, 22.79, 25.20 (1:1:2:2:1, 7C, CH pentyl), 27.04–27.56, 28.98 (28C, CH₂ pentyl), 48.38 (NCH₃), 52.54 (NCH₃), 59.21 (NCH₂), 63.54 (NCH₂), 135.60 (d, C₆F₅ meta, *J*_{FC} = 237 Hz), 147.75 (d, C₆F₅ ortho, *J*_{FC} = 231 Hz). The signals assigned as ipso and para carbons were not observed, due to low intensity. ²⁹Si{¹H} NMR (79 MHz, CDCl₃, 0.02 M Cr(acac)₃, room temperature): δ -56.49, -56.88, -65.17, -65.69, -68.34 (1:2:1:1:2). IR data (KBr): 3350 (br, w), 2949 (s), 2867 (s), 1500 (m), 1456 (s), 1246 (m), 1100 (vs), 959 (s), 909 (m), 808 (m), 789 (w), 770 (w), 730 (w), 505 (m) cm⁻¹.

Preparation of [Pd{(c-C₅H₉)₇Si₇O₁₀(OH)₂}(C₆H₃F₂-2,4)(tmeda)] (5). To a solution of [PdI(C₆H₃F₂-2,4)(tmeda)] (46 mg, 0.10 mmol) in toluene (5 mL) were added (c-C₅H₉)₇Si₇O₉(OH)₃ (87 mg, 0.10 mmol) and Ag₂O (28 mg, 0.12 mmol). The reaction mixture was stirred at room temperature for 10 days. After completion of the reaction the gray suspension was filtered through Celite. The solvent was evaporated under reduced pressure, and 1 mL of hexane was added to the crude product. The solution was cooled to -20 °C to give **5** as a pale yellow solid (89 mg, 74%). An analogous reaction was performed at 60 °C for 24 h and afforded the same product **5**. Anal. Calcd for C₄₇H₈₄F₂N₂O₁₂PdSi₇: C, 46.65; N, 2.31; F, 3.14; H, 7.00. Found: C, 46.31; N, 2.23; F, 3.20; H, 6.88. Dec pt: 162 °C. ¹H NMR (400 MHz, CDCl₃, room temperature): δ 0.96 (m, 7H, CH pentyl), 1.1–2.8 (m, 72H, CH₂ pentyl and tmeda), 6.39 (m, 1H, C₆H₃F₂ meta, *J*_{HH} = 8 Hz, *J*_{HF} = 3 Hz), 6.59 (m, 1H, C₆H₃F₂ meta', *J*_{HH} = 8 Hz, *J*_{HF} = 3 Hz), 7.28 (m, 1H, C₆H₃F₂ ortho, *J*_{HH} = 8 Hz, *J*_{HF} = 5 Hz), 8.2 (br, 2H, OH). ¹H NMR (400 MHz, C₇D₈, room temperature): δ 1.1–1.4 (m, 7H, CH pentyl), 1.4–2.1 (m, 72H, CH₂ pentyl and tmeda), 6.54 (m, 1H, C₆H₃F₂ meta), 6.90 (m, 1H, C₆H₃F₂ meta), 7.50 (m, 1H, C₆H₃F₂ ortho), 8.18 (br, 1H, OH), 8.55 (br, 1H, OH). ¹⁹F{¹H} NMR (376 MHz, C₇D₈, room temperature): δ -96.7 (br, F_o), -122.0 (m, F_p). ¹³C-{¹H} NMR (100 MHz, CDCl₃, room temperature): δ 22.50, 22.59, 23.06, 25.16 (2:2:2:1, 7C, CH pentyl), 27.06–27.66, 28.89 (28C, CH₂ pentyl), 47.94 (N(CH₃)), 52.04 (br, N(CH₃)), 58.34 (NCH₂), 63.55 (NCH₂), 101.45* (dd, C₆H₃F₂ meta, ²*J*_{CF} = 33 Hz, ²*J*_{CF} = 24 Hz), 109.57 (d, C₆H₃F₂ ipso, ²*J*_{CF} = 19 Hz), 122.73* (d, C₆H₃F₂ meta', ²*J*_{CF} = 40 Hz), 138.47* (dd, C₆H₃F₂ ortho', ³*J*_{CF} = 19 Hz, ³*J*_{CF} = 7.4 Hz), 161.05 (dd, C₆H₃F₂ para or ortho, *J*_{CF} = 240 Hz, ³*J*_{CF} = 12 Hz), 164.63 (dd, C₆H₃F₂ para or ortho, *J*_{CF} = 230 Hz, ³*J*_{CF} = 11 Hz). Signals marked with an asterisk were assigned by 2D dimensional NMR spectroscopy. ²⁹Si{¹H} NMR (79 MHz, CDCl₃, 0.02 M Cr(acac)₃, room temperature): δ -55.3, -55.6, -56.1, -65.3, -65.8, -66.4 (1:1:1:2:1:1). IR data (KBr): 3300 (br, w), 2949 (s), 2865 (s), 1590 (w), 1468 (m), 1389 (w), 1258 (m), 1100 (vs), 955 (m), 909 (w), 843 (w), 804 (m), 770 (w), 730 (w), 502 (m) cm⁻¹.

X-ray Crystallography. Crystals of **4** suitable for X-ray diffraction study were mounted on a glass capillary tube. The data were collected to a maximum 2θ value of 55.0°. A total of 720 oscillation images were collected on a Rigaku Saturn CCD area detector equipped with monochromated Mo Kα radiation (λ = 0.710 73 Å) at -160 °C. A sweep of data was done using ω scans from -110.0 to 70.0° in 0.5° steps, at χ = 45.0° and φ = 0.0°. The detector swing angle was -20.42°. A second sweep was performed using ω scans from -110.0° to 70.0° in 0.5° step, at χ = 45.0° and φ = 90.0°. The crystal-to-detector distance was 44.84 mm. Readout was performed in the 0.070 mm pixel mode. Calculations were carried out by using the program package Crystal Structure, version 3.7 for Windows. A full-matrix least-squares refinement was used for the non-hydrogen atoms with anisotropic thermal parameters. Hydrogen atoms except for the OH hydrogens of **4** were located by assuming the ideal geometry and were included in the structure calculation without further refinement of the parameters. Crystallographic data and details of refinement are summarized in Table 2.

Acknowledgment. N.M. thanks the Japanese Society for Promotion of Science for a postdoctoral fellowship for foreign researchers (2004–2006). This work was financially supported by a Grant-in-Aid for Scientific Research for Young Chemists (No. 17750049) and for Scientific Research on Priority Areas, from the Ministry of Education, Culture, Sport, Science, and Technology Japan, and by the 21st Century COE Program “Creation of Molecular Diversity and Development of Functionalities”.

Supporting Information Available: Crystallographic data for **4** as a CIF file. This material is available free of charge via the Internet at <http://pubs.acs.org>.

OM0610492